

Bulk etch characteristics of colorless LR 115 SSNTD

K.C.C. Tse, F.M.F. Ng, D. Nikezic, K.N. Yu *

Department of Physics and Materials Science, City University of Hong Kong, Tat Chee Avenue, Kowloon Tong, Hong Kong

Available online 13 May 2007

Abstract

The colorless LR 115 solid-state nuclear track detector (SSNTD) (from DOSIRAD) is based on cellulose nitrate and was first studied in view of its applicability in radiobiological experiments with alpha particles. In this paper, the bulk etch characteristics were studied. We first showed that the shape of the alpha-particle tracks are irregular with blurred contours under the optical microscope. This has made measurements of track diameters very difficult. The phenomenon was explained in terms of the roughness of the detectors. As a result, the common method used to determine the bulk etch rates through measurements of opening diameters of tracks is not valid. We then proposed the surface profilometry method for determination of the removed active-layer thickness during etching. The bulk etch rates with 2.5 N aqueous solution of NaOH as the etchant, with and without magnetic stirring were determined for etching temperatures of 40, 50 and 60 °C. The data supported the Arrhenius type equation. The corresponding activation energies were determined. Finally, relationships were derived between the residual active-layer thickness and the infrared transmittances at different wave numbers. The infrared transmittances were found useful in revealing the active-layer thickness of the colorless LR 115 SSNTD, the correlations being described by quadratic relationships.

© 2007 Elsevier B.V. All rights reserved.

PACS: 29.40; 23.60

Keywords: Solid-state nuclear track detector; SSNTD; LR 115; Bulk etch

1. Introduction

The red LR 115 detector (from DOSIRAD) is based on cellulose nitrate and is a commonly used solid-state nuclear track detector (SSNTD). The chemical composition of cellulose nitrate is shown in Fig. 1. A most recent review of SSNTDs can be found in [1]. Another type of LR 115 SSNTD from DOSIRAD, which is also based on cellulose nitrate and is colorless, was first studied in view of its applicability in radiobiological experiments with alpha particles [2]. Other than [2], there are no other studies on this colorless LR 115 SSNTD. Before the colorless LR 115 SSNTD can be widely used for radiobiological experiments, its properties should be studied in more details. Among other information, the bulk etch characteristics will be vital in the practical use of this type of SSNTD in radiobiological

experiments. The present paper is devoted to determine the bulk etch rates of the colorless LR 115 SSNTD under different etching conditions, which are then generalized in the form of an activation energy in the Arrhenius equation.

The determination of the bulk etch rates for the colorless LR 115 SSNTD is not as straightforward as those for other SSNTDs. The most common method to determine the bulk etch rates in SSNTDs (such as the red LR 115 or CR-39 detector) is through measurements of opening diameters of tracks generated by normally incident heavy ions. However, it will be shown in Section 2 that the track openings are not sufficiently sharp in the colorless LR 115 SSNTD to provide accurate measurements. Therefore, in Section 3, we have to explore the surface profilometry method for determination of the removed active-layer thickness during etching to calculate the bulk etch rates [3,4]. The bulk etch rates for different etching conditions will then be measured, and the activation energy will be determined.

* Corresponding author. Tel.: +852 27887812; fax: +852 27887830.
E-mail address: peter.yu@cityu.edu.hk (K.N. Yu).

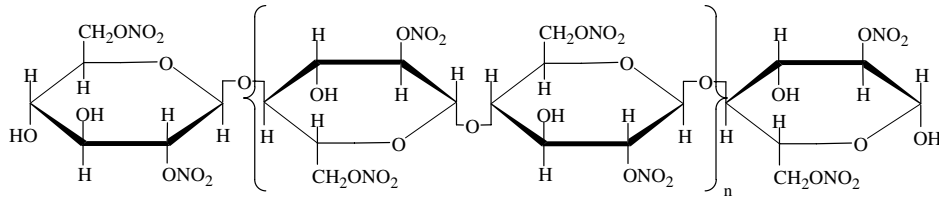


Fig. 1. Chemical formula for cellulose nitrate (adopted from [6]).

Finally, in Section 4, we will also establish the relationship between infrared transmittances at different wave numbers and the residual active-layer thickness. This will provide a fast and non-destructive method for measuring the amount of bulk etch in the future. The infrared transmittances at different wave numbers will also be explained by the presence of different functional groups as well as modes of vibrations in the SSNTD.

All the colorless LR 115 detectors used in this project were purchased from DOSIRAD. The detectors consist of an active layer of cellulose nitrate on a 100 μm polyester base.

2. Track diameters

As mentioned in Section 1, the most common method to determine the bulk etch rates in SSNTDs is through measurements of opening diameters of tracks generated from normally incident heavy ions. Therefore, in this section, the practicality of measuring track diameters in colorless LR 115 SSNTD will first be examined. The LR 115 detectors were irradiated with alpha particles with energies of 1, 1.5, 2 and 3 MeV under normal incidence through a collimator. The alpha source employed in the present study was a planar ^{241}Am source (main alpha energy = 5.49 MeV under vacuum). Normal air was used as the energy absorber to control the final alpha energies incident on the detector. A relationship between the alpha energy and the air distance traveled by an alpha particle was therefore needed. This relationship was obtained by measuring the energies for alpha particles passing different distances through normal air using α spectroscopy systems (ORTEC Model 5030) with passivated implanted planar silicon (PIPS) detectors of areas of 300 mm^2 .

After irradiation, the detectors were etched in 2.5 N aqueous solution of NaOH. The etching temperatures were 40 $^\circ\text{C}$ for irradiation with 3 MeV alpha particles, and 50 $^\circ\text{C}$ for irradiation with 1, 1.5 and 2 MeV alpha particles. The temperature was kept constant with an accuracy of ± 1 $^\circ\text{C}$. The detectors were etched using a magnetic stirrer (Model No.: SP72220-26, Barnstead/Thermolyne, Iowa, USA) for more uniform etching [4]. After chemical etching, the detectors were taken out from the etchant, rinsed with distilled water and dried in air. An optical microscope in the transmission mode together with an image analyzer were used to measure the dimensions of the tracks.

Fig. 2(a) shows the images of 1-MeV alpha-particle tracks in colorless LR 115 detectors after etching at 40 $^\circ\text{C}$

for 70 and 100 min. It can be seen that the shape of the alpha-particle tracks were in fact irregular with blurred contours thus making accurate measurements of track diameters very difficult. The ragged edge of the etched-track openings, as well as the rough surface of the detector were observed in the image. It became more difficult to focus on the openings of the track for increasing etching time.

The blurred images are explained in terms of the roughness of the etched detector surface. Atomic force microscope (AFM) has been applied to evaluate the surface roughness of the colorless LR 115 SSNTDs. The AFM used in the present project was the Autoprobe CP model from Park Scientific Instruments (1171 Borregas Avenue, Sunnyvale, CA 94089). The probe of the AFM employed was an Ultralever, with an opening angle of 10 $^\circ$ and a length of 4 μm . Contact mode operation was used where high-resolution image was expected. A constant force of 13.2 nN was applied on the tip and the scan rate was 1 Hz. The surfaces of the detectors were imaged directly in air and room temperature. The LR 115 detectors which have been etched at temperatures 40, 50 and 60 $^\circ\text{C}$ for different etching periods are scanned for an area of 20 \times 20 μm^2 with a 256 \times 256 pixel resolution to determine the root-mean-square (rms) roughness of the detector surface.

Fig. 2(b) shows the AFM images of the colorless LR 115 detector surface after etching at 40 $^\circ\text{C}$ for 70 and 100 min. The rms roughness values recorded by AFM were 0.0273 and 0.112 μm for etching time of 70 and 100 min, respectively. It is therefore seen that the etched surfaces of colorless LR 115 SSNTDs were rough and became more so for longer etching. This explains the difficulty of defining the track openings in colorless LR 115 SSNTDs, particularly for long etching times.

Fig. 3 shows the variation of rms roughness recorded by AFM as a function of etching time for a scanned area of 20 \times 20 μm^2 . The surface roughness was nearly the same for all etching temperatures when the detectors were etched down to a residual active-layer thickness of 9 μm . The residual active-layer thickness is measured through infrared measurements as described in Section 4. When the active layer was smaller than 9 μm , the rms roughness was lower for 60 $^\circ\text{C}$ as compared to those for 40 and 50 $^\circ\text{C}$. This is explained by the longer etching time required for lower etching temperatures for the same removed active layer. The etching time was thus identified as an important factor affecting the surface roughness. On the other hand, for the same etching temperature, the surface roughness increases as the residual active-layer thickness decreases. The detector

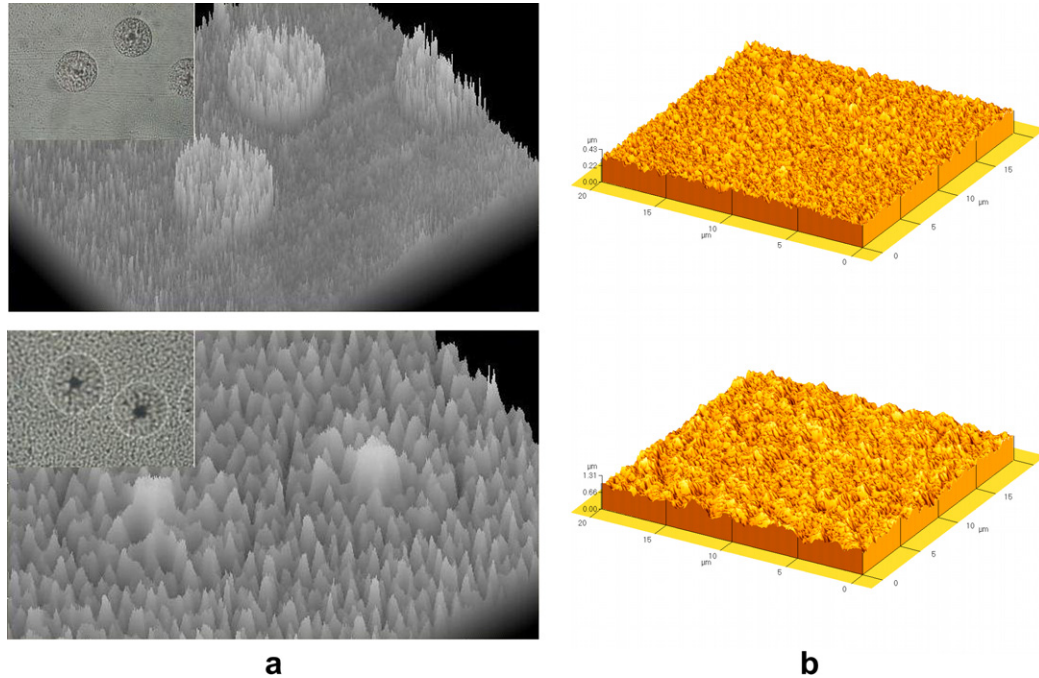


Fig. 2. (a) Images of 1-MeV alpha-particle tracks in colorless LR 115 detectors after etching at 40 °C for 70 min (above) and 100 min (below). The inserts show the images recorded under the optical microscope in the transmission mode, while the larger images are produced using the software National Instruments IMAQ Vision Builder 6.1 (peaks in the images representing troughs in the real world). (b) The corresponding images of the colorless LR 115 detector surface recorded using atomic force microscope (AFM). The RMS roughness values recorded by AFM were 0.0273 and 0.112 μm for etching time of 70 and 100 min, respectively.

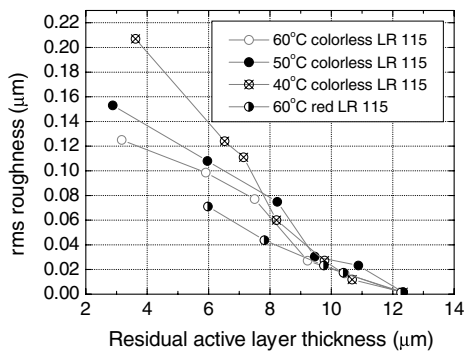


Fig. 3. Variation of root-mean-square (rms) roughness of the surface of colorless LR 115 detectors (recorded using AFM) as a function of residual thickness at 40, 50 and 60 °C and that of red LR 115 as a function of residual thickness at 60 °C.

roughens as a result of chemical etching. One observation is that the colorless LR 115 SSNTD becomes much rougher than the red LR 115 SSNTD upon etching. The exact reason behind this phenomenon is unknown. However, because of this, it is more difficult to distinguish the alpha-particle tracks from stain marks and scratches for the colorless LR 115 SSNTD than that for the red LR 115 SSNTD.

3. Surface profilometry and bulk etch rate

We have shown in Section 2 that track openings are not sufficiently sharp in the colorless LR 115 SSNTD to enable

accurate measurements. Therefore, we have to explore the surface profilometry method for determination of the removed active-layer thickness during etching to calculate the bulk etch rates. In particular, we will determine the dependence of the bulk etch rate V_b of the colorless LR 115 on the etching temperature as well as on the presence of magnetic stirring during etching. A total of five detectors were used for each studied conditions.

The procedures for measuring the active-layer thickness followed those described in [3,4]. Before etching, a small portion of the active layer was first removed by a razor to expose the polyester base. After etching, a surface profilometer called Form Talysurf PGI (Taylor Hobson, Leicester, England) was employed to measure the active-layer thickness. The measuring system is based on a laser interferometric transducer. A computer-controlled stylus passes slowly across a surface of interest during measurements, while the data are processed by the computer to generate an output graph showing the profile of the scanned surface. The mean value and the standard deviation for the active-layer thickness were obtained through measurements for five different positions of the cliff.

The detectors were etched in a 2.5 N aqueous solution of NaOH at three different temperatures, namely, 40, 50 and 60 °C, for both the presence and absence of magnetic stirring. It is expected that magnetic stirring can provide a faster and more uniform etching [4]. For each studied etching temperature, LR 115 detectors were removed from the etchant at different etching periods and then immediately

rinsed with distilled water. After drying, the active-layer thickness was measured using surface profilometry.

The results on the residual active-layer thickness (μm) as a function of the etching time for different temperatures (40, 50 and 60 °C) with and without stirring are shown in Fig. 4. Linear relationships are observed. By fitting the linear relationship $y = A + Bx$ to the experimental data, where y (μm) is the thickness of the active layer and x (min) is the etching period, the bulk etch rates for the colorless LR 115 can be determined for different etching conditions, which are shown in Table 1.

The activation energy E_a is the energy required in activating the reaction between the detector material and the etching solution. Generally speaking, the dependence of the bulk etch rate V_b of SSNTDs depends on the etching temperature T through an Arrhenius type equation:

$$V_b = A \exp\left(-\frac{E_a}{kT}\right). \quad (1)$$

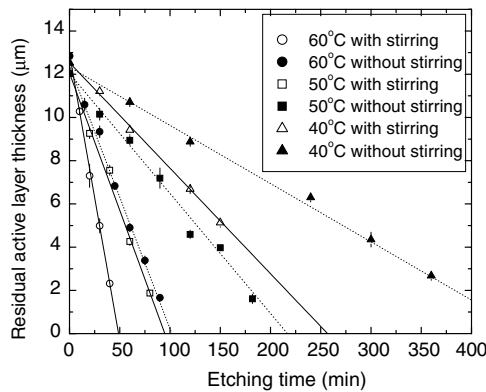


Fig. 4. The relationship between the residual active-layer thickness (μm) and the etching time for different temperatures (40, 50 and 60 °C) with and without stirring.

Table 1

The coefficients (A and B) for the linear regression equations ($y = A + Bx$) for the relationship between the residual active-layer thickness (μm) (y) and the etching time (x) for different temperatures (40, 50 and 60 °C) with and without stirring, and the corresponding determined etching rates ($\mu\text{m h}^{-1}$)

Temperature (°C)	With stirring	Without stirring
60	$A = 12.93 \pm 0.03$ $B = -0.2651 \pm 0.0019$ Etching rate = $15.9 \pm 0.1 \mu\text{m h}^{-1}$	$A = 12.38 \pm 0.22$ $B = -0.1216 \pm 0.0042$ Etching rate = $7.30 \pm 0.25 \mu\text{m h}^{-1}$
50	$A = 12.05 \pm 0.14$ $B = -0.1270 \pm 0.0032$ Etching rate = $7.62 \pm 0.19 \mu\text{m h}^{-1}$	$A = 12.03 \pm 0.20$ $B = -0.05547 \pm 0.00190$ Etching rate = $3.33 \pm 0.11 \mu\text{m h}^{-1}$
40	$A = 12.53 \pm 0.06$ $B = -0.0488 \pm 0.0006$ Etching rate = $2.93 \pm 0.03 \mu\text{m h}^{-1}$	$A = 2.33 \pm 0.17$ $B = -0.02693 \pm 0.00110$ Etching rate = $1.62 \pm 0.07 \mu\text{m h}^{-1}$

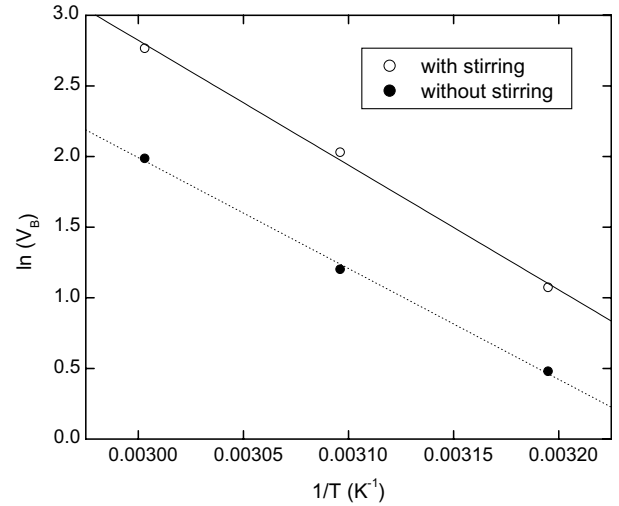


Fig. 5. The data and the corresponding linear regression lines for etching the colorless LR 115 SSNTDs in 2.5 N aqueous NaOH at 40, 50 and 60 °C for the presence of magnetic stirring (open circles and solid line) and absence of magnetic stirring (filled circles and dotted line).

In this way,

$$\ln V_b = \ln A - \frac{E_a}{kT}, \quad (2)$$

so E_a can be obtained from the slope of the relationship between $\ln(V_b)$ and $1/T$. The data for etching the colorless LR 115 SSNTDs in 2.5 N aqueous NaOH at 40, 50 and 60 °C for both the presence and absence of magnetic stirring are shown in Fig. 5. Linear relationships between $\ln(V_b)$ and $1/T$ are apparent for both the presence and absence of magnetic stirring.

By fitting the linear relationship $\ln(V_b) = C + D(1/T)$ to the experimental data, we obtain:

with stirring

$$C = 29.3 \pm 1.6; D = -8830 \pm 500, \\ E_a = 0.761 \pm 0.043 \text{ eV},$$

without stirring

$$C = 25.5 \pm 1.0; D = -7850 \pm 330, \\ E_a = 0.676 \pm 0.028 \text{ eV}.$$

4. Residual active-layer thickness and FTIR transmittance

Although surface profilometry is a fast and accurate method for determining the active-layer thickness and thus the bulk etch rate for the LR 115 SSNTD, the method is destructive. In a previous work, Ng et al. [5] proposed to measure the thickness of the active layer of the red LR 115 SSNTD by using Fourier Transform Infrared (FTIR) spectroscopy, with the wave number at 1598 cm^{-1} corresponding to the O–NO₂ bond. They found an exponential decay relationship between the infrared transmittance at the wave number at 1598 cm^{-1} and the thickness of the

active layer for the red LR 115 detector. This has provided a fast and non-destructive method to measure the thickness of removed layer from etching of the red LR 115 detector.

Here, we would extend the method to the colorless LR 115 SSNTD. In order to identify the appropriate wave-number(s) that can be used for the correlation study, the first task was to obtain the FTIR spectrum of the unetched colorless LR 115 SSNTD (with the polyester base). The FTIR spectroscopy system employed for the present research was the Perkin Elmer Model 16 PC FT-IR system. Each detector was scanned for 10 cycles to give the spectrum. The studied wave numbers range between 4000 and 400 cm^{-1} .

The FTIR spectrum of the unetched colorless LR 115 SSNTD is shown in Fig. 6. It is characterized by absorption at the following wave numbers (cm^{-1}): 2907 [C–H stretch], 1614 [–ONO₂–], 1524 [N–O asymmetric stretch], 899 [CCO– stretch], 680 [NO₂ deformation vibration], 632 [–OH out of plane deformation vibration] and 520 [NO₂ rocking vibration], with the corresponding functional groups/modes of vibration shown in square brackets after the wave numbers. The wave numbers corresponding to these absorptions (transmission troughs), and the corresponding assignment of the function groups and the modes of vibration are shown in Table 2. The infrared transmittance at these wave numbers will be studied for different residual active-layer thickness.

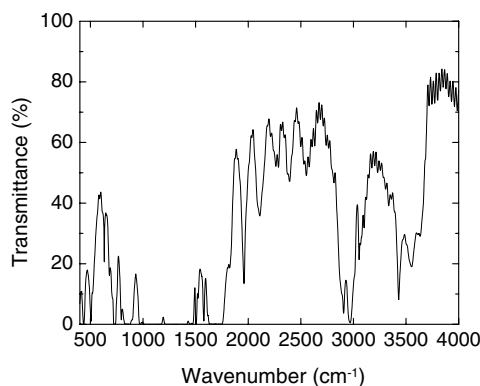


Fig. 6. The FTIR spectrum of a piece of unetched colorless LR 115 SSNTD (with the polyester base).

Table 2

The wave numbers of the more significant absorption peaks (transmission troughs) in the FTIR spectrum of the unetched colorless LR 115 SSNTD (see Fig. 6), and the corresponding assignment of the function groups and the modes of vibration

Position of the peak (cm^{-1})	Functional group/modes of vibration
2907	C–H stretch
1614	–ONO ₂ –
1524	N–O asymmetric stretch
899	CCO– stretch
680	NO ₂ deformation vibration
632	–OH out of plane deformation vibration
520	NO ₂ rocking vibration

Before etching, a small portion of the active layer was first removed by a razor to expose the polyester base. At different etching periods, detectors were removed from the etchant and immediately rinsed by distilled water. After drying, the portions of the detectors with the active layer were scanned using FTIR spectroscopy. The scanned diameter was 9 mm so the scanned area was 0.64 cm^2 .

To establish the correlation between the infrared transmittance and the thickness of the active layer of the LR 115 detector, the active-layer thickness should be accurately determined. Here, surface profilometry was used as described in Section 3. For each detector, the mean value of the residual active-layer thickness and the associated standard deviation were obtained from measurements at six different positions of the cliff (edge of the active layer over the exposed base).

The relationships between the FTIR transmittance (%) and the measured active-layer thickness (μm) for different wave numbers are shown in Fig. 7. Anti-correlations between the active-layer thickness and the FTIR transmittance at different wave numbers were established. Fig. 7 shows that the FTIR transmittances at the studied wave numbers, in particular 680 and 632 cm^{-1} , can be used to reveal the active-layer thickness of the colorless LR 115 SSNTD. The data are fitted by the quadratic relationship $y = Fx^2 + Gx + H$, where y is the thickness of active layer and x is the corresponding FTIR transmittance. The fitting results are shown in Table 3.

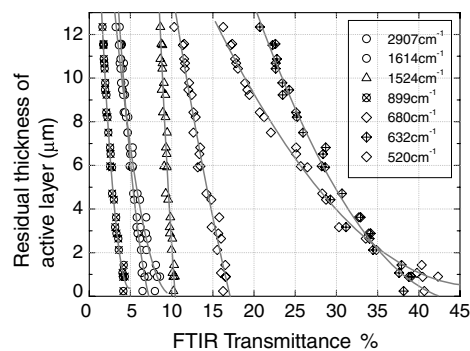


Fig. 7. Relationship between the active-layer thickness and the corresponding FTIR transmittance at different wave numbers.

Table 3

Quadratic relationships between the active-layer thickness y and the FTIR transmittance x at different wave numbers, and the corresponding R^2

Wave number (cm^{-1})	Quadratic relationship	R^2
2907	$y = 0.607x^2 - 10.235x + 42.301$	0.986
1614	$y = 0.285x^2 - 5.583x + 27.583$	0.986
1524	$y = 0.824x^2 - 22.928x + 149.480$	0.968
899	$y = 1.058x^2 - 10.550x + 26.505$	0.994
680	$y = 0.013x^2 - 1.183x + 27.784$	0.991
632	$y = 0.023x^2 - 2.034x + 44.842$	0.986
520	$y = 0.042x^2 - 3.116x + 41.004$	0.966

5. Conclusions

- (1) In colorless LR 115 detectors, the shape of the alpha-particle tracks are irregular with blurred contours under the optical microscope. This has made measurements of track diameters very difficult. Through the root-mean-square (rms) roughness of the detector surface revealed by atomic force microscope (AFM) studies, it is concluded that the etched surfaces of colorless LR 115 SSNTDs are rough and become more so for longer etching. This explains the difficulty of defining the track openings in colorless LR 115 SSNTDs, particularly for long etching times. As a result, the common method to determine the bulk etch rates through measurements of opening diameters of tracks is not valid for colorless LR 115 SSNTDs.
- (2) The surface profilometry method is then proposed for determination of the removed active-layer thickness during etching to calculate the bulk etch rates with 2.5 N aqueous solution of NaOH as the etchant. The bulk etch rates with magnetic stirring are 2.93, 7.62 and 15.9 $\mu\text{m h}^{-1}$ for etching at 40, 50 and 60 °C, respectively; while those without magnetic stirring are 1.62, 3.33 and 7.30 $\mu\text{m h}^{-1}$ for etching at 40, 50 and 60 °C, respectively. The data show evidence that the bulk etch rate depends on the etching temperature through an Arrhenius type equation, with the activation energies given by 0.761 and 0.676 eV for the presence and absence of magnetic stirring, respectively.
- (3) Finally, relationships have been derived between the residual active-layer thickness and the infrared transmittances at different wave numbers. The FTIR

spectrum of the unetched colorless LR 115 SSNTD is characterized by absorption at the following wave numbers (cm^{-1}): 2907 [C–H stretch], 1614 [–ONO₂–], 1524 [N–O asymmetric stretch], 899 [CCO– stretch], 680 [NO₂ deformation vibration], 632 [–OH out of plane deformation vibration] and 520 [NO₂ rocking vibration], with the corresponding functional groups/modes of vibration shown in square brackets after the wave numbers. The infrared transmittance at these wave numbers were found useful in revealing the active-layer thickness of the colorless LR 115 SSNTD, the correlations being described by quadratic relationships.

Acknowledgment

The present research is supported by the CERG grant CityU 102803 from the Research Grant Council of Hong Kong.

References

- [1] D. Nikezic, K.N. Yu, Mater. Sci. Eng. R 46 (2004) 51.
- [2] B. Dörschel, D. Hermsdorf, S. Pieck, S. Starke, H. Thiele, F. Weickert, Nucl. Instr. Meth. B 207 (2003) 154.
- [3] D. Nikezic, A. Janicijevic, Appl. Radiat. Isotopes 57 (2002) 275.
- [4] C.W.Y. Yip, J.P.Y. Ho, V.S.Y. Koo, D. Nikezic, K.N. Yu, Radiat. Meas. 37 (2003) 197.
- [5] F.M.F. Ng, C.W.Y. Yip, J.P.Y. Ho, D. Nikezic, K.N. Yu, Radiat. Meas. 38 (2004) 1.
- [6] R. Barillon, M. Fromm, A. Chambaudet, R. Katz, J.P. Stoquert, A. Pape, Radiat. Meas. 31 (1999) 71.